Different Time Scales in Wave Function Intensity Statistics

D. A. Wisniacki,[1,2] F. Borondo,[1,*] E. Vergini,[2] and R. M. Benito[3]

[1]*Departamento de Química C–IX, Universidad Autónoma de Madrid, Cantoblanco, 28049–Madrid (Spain).*
[2]*Departamento de Física, Comisión Nacional de Energía Atómica. Av. del Libertador 8250, 1429 Buenos Aires (Argentina).*
[3]*Departamento de Física, E.T.S.I. Agrónomos, Universidad Politécnica de Madrid, 28040 Madrid (Spain).*
(Dated: November 14, 2018)

Unstable periodic orbits scar wave functions in chaotic systems. This also influences the associated spectra, that follow the otherwise universal Porter–Thomas intensity distribution. We show here how this deviation extend to other longer periodic orbits sharing some common dynamical characteristics. This indicates that the quantum mechanics of the system can be described quite simply with few orbits, up to the resolution associated to the corresponding length.

PACS numbers: PACS numbers: 05.45.-a, 03.65.Sq, 05.45.Mt

Chaos is a well defined phenomenon in classical mechanics, but its manifestations at quantum level are not fully understood yet [1]. The pioneering work of Gutzwiller [2], showing how the eigenvalues density of chaotic systems can be obtained from classical periodic orbits (PO), constitutes an important landmark in the investigation of "quantum chaos". Later Heller demonstrated that, contrary to reasonable conjectures, unstable POs have a profound influence in the distribution of quantum probability density of a non–vanishing class of wave functions, which appear highly localized over these classical paths [3]. The wave functions exhibiting this localization are said to be "scarred", and they play a very important role in semiclassical theories [4]. Recently, several methods, based on very different strategies, have been described in the literature [5, 6] for the systematic construction of non–stationary wave functions highly localized on POs. These novel tools also provide new insight towards the understanding of the role of scarring in the quantum mechanics of chaotic systems [7]. Scars also condition spectra. Recurrences in the correlation function originated by the linearized dynamics around unstable POs are the reason for the existence of marked low resolution structure in the spectra of chaotic systems. Heteroclinic orbits have also been demonstrated to be important when extending this theory beyond the linearized regime [8, 9].

Another main achievement in quantum chaos is undoubtedly Random Matrix Theory (RMT) [10], which accounts for many properties in the quantum spectra of chaotic systems, such as the widespread nearest neighbor energy level spacing, which for all strong mixing systems follows the Wigner surmise [11]. The beauty of many RMT results is their universality, which turns out to be also its drawback, since they are independent of the initial state preparation details and its dynamics. Other measures sensitive to them, such as the distribution of spectral intensities, seem then, in principle, better suited to elucidate relevant features in a given spectrum. However, the statistical fluctuations of quantum transition strengths in stochastic systems was also found to be de-

scribed by another RMT universal formula, the Porter–Thomas (PT) distribution [12]. In this respect, Alhassid and Levine demonstrated [13] that the PT distribution can be simply obtained from the principle of maximum entropy of the strength distribution, with the only constrain of the ever present sum rule for the total strength of the transition. Sibert and Borondo [14] showed that the same result can be derived by imposing the dynamical constrains implied by the short time motion of the system. Later Kaplan [15] found that, although the tail of wave function intensity distribution in phase space is dominated by scarring associated with the least unstable PO, when the low resolution modulation induced by it is removed, the remaining distribution matchs the standard PT expression.

In this Letter we report an study on the intensity distribution statistics for the stadium scar wave functions, calculated with the method of Ref. 5. We show that the information contained in it about POs is far richer than assumed in the previously existing literature [10, 14, 15], actually extending to times much longer than that of the local short term dynamics dictated by the least unstable PO. However, this view is based on few POs, thus representing an important conceptual simplification over other approaches (see for example [8, 9]), which can be very useful in future developments of scar theory.

In our study we use a system consisting of a particle of mass $1/2$ enclosed in a desymmetrized stadium billiard of radius $r = 1$ and area of $1 + \pi/4$, with Newman boundary conditions on the symmetry axes (only even–even parity eigenfunctions will be considered).

We consider the dynamics influenced by the horizontal PO running along the x axis with $y = 0$. For this purpose we start from a symmetry adapted initial wave packet:

$$
\begin{aligned}
\langle x, y | \phi(0) \rangle &= a G_{x^0, y^0, P_x^0, P_y^0} + b G_{-x^0, y^0, -P_x^0, P_y^0} \\
&\quad + c G_{x^0, -y^0, P_x^0, -P_y^0} \\
&\quad + d G_{-x^0, -y^0, -P_x^0, -P_y^0} + \text{c.c.}
\end{aligned}
\tag{1}
$$

where

$$G_{\mathbf{q^0},\mathbf{P^0}} = \prod_j (\pi\alpha_j^2)^{-1/4} e^{-(q_j-q_j^0)^2/2\alpha_j^2} e^{iP_j^0(q_j-q_j^0)}, \quad (2)$$

(the coefficients $a, b, c,$ and d are obtained by imposing Newman boundary conditions at the symmetry axes), and compute the (infinite resolution) spectrum

$$I_\infty(E) = \sum_n |\langle n|\phi(0)\rangle|^2 \delta(E-E_n), \quad (3)$$

with $(x^0, y^0, P_x^0, P_y^0)=(1,0,k_0,0)$ and $\alpha_x=\alpha_y=1.603/k_0^{1/2}$ ($\hbar$ is set equal to 1 throughout this paper). Kets $|n\rangle$ represent the eigenstates of the system, which have been obtained using the scaling method [16]. The aspect of the obtained $I_\infty(E)$ is rather irregular (see results below), due to the highly chaotic nature of the dynamics in this system. However, when examined closely, the contributing "sticks" are seen to come grouped in clumps. This indicates the existence of a clear underlying structure, which is due to recurrences in the associated correlation function, $C(t) = \langle\phi(0)|\phi(t)\rangle$, induced by the horizontal PO used to select the initial position of the wave packet. This regularity shows up as well defined bands in the low resolution version of the spectrum, $I_T(E)$,

$$I_T(E) = \frac{1}{2\pi} \int_{-\infty}^{\infty} dt\, W_T(t) C(t) \exp(iEt), \quad (4)$$

where $W_T(t)$ is a suitable smoothing window function, filtering out the dynamics of the system for times longer than T. Moreover, the positions of these bands are given by the usual Bohr–Sommerfeld quantization condition,

$$k_m = \frac{2\pi}{L_\mu}\left(m + \frac{\nu_\mu}{4}\right), \quad (5)$$

with $L_\mu=4$ and $\nu_\mu=3$. The wave functions associated to these bands correspond to a series of scar functions on the PO with an increasing excitation along it, as discussed elsewhere [5, 17, 18].

To efficiently study the characteristics of the spectra corresponding to this band structure we define a "scar spectrum" in the following way. Using the procedure described above, we calculate spectra at all energies, $k_0=k_m$, quantized with the Bohr–Sommerfeld formulae and construct a new spectrum, $\tilde{I}_\infty(E)$, by taking only the central clump from each one of them:

$$\tilde{I}_\infty(E) = \sum_m I_m^{\text{band}} = \sum_m \sum_{\{E_n\}}{}' |a_n^m|^2\, \delta(E-E_n), \quad (6)$$

where the prime indicates that the sum is only carried out for states in the range $(E_m-E_{m-1})/2 < E_n < (E_{m+1}-E_m)/2$. In this way the spectrum statistics is improved, since the constrain imposed by the finite width of the initial wave packet is eliminated. Our calculations were
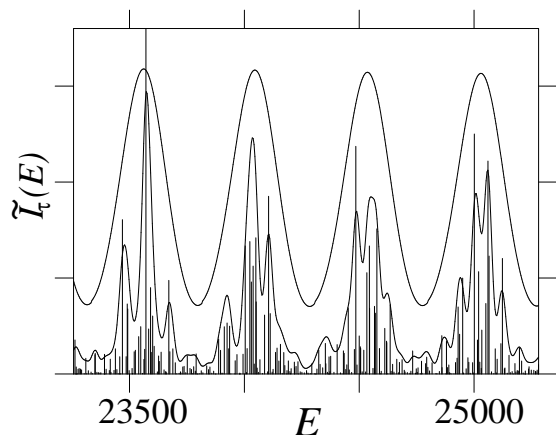

FIG. 1: Scar spectrum, $\tilde{I}_\tau(E)$, at infinite (stick) and low resolution: $\tau = 1$ and 4.5 (solid lines), corresponding to a wave packet initially centered on the horizontal axis of a desymmetrized stadium billiard with $r = 1$, area $1 + \pi/4$, and Newman boundary conditions at the symmetry axes.

performed in the range k=50–250, which includes approximately 8400 stadium eigenstates. Similarly to what was done in eq. (4), we can now define a low resolution version of this spectrum which, for a Gaussian window function, takes the form

$$\tilde{I}_\tau(E) = 2\tau T_0 \pi^{-1/2} \sum_{\{E_n\}}{}' |a_n|^2\, e^{-2\tau^2 T_0^2(E-E_n)^2}, \quad (7)$$

where τ is an adimensional smoothing parameter and T_0 the period of the scarring orbit. The corresponding results, in the range E=23250–25300, are shown in Fig. 1, for τ=1 and 4.5. The first value of the smoothing parameter corresponds approximately to the smallest smoothing which washes out all substructures. The required time scales with the inverse of the Lyapunov exponent [3]. When the resolution is increased to τ=4.5 another superimposed intra–band structure is then exposed, thus revealing the relevance of longer time dynamics.

To quantitatively examine the implication of this result, we consider next the statistics of intensities in our scar spectrum. According to RMT the distribution of "dynamically normalized" intensities in a fully chaotic system is given by the usual χ^2 (PT) fluctuations [12],

$$P(x) = (2\pi x)^{-1/2} e^{-x/2}. \quad (8)$$

However, and as stated in the introduction, one crucial point when performing this analysis is to eliminate the modulation due to any obvious low resolution structure present in the spectrum, so that all intensities are compared on the same relative scale. This can be acomplished by "renormalizing" the intensities with the corresponding value of the envelope [14, 15],

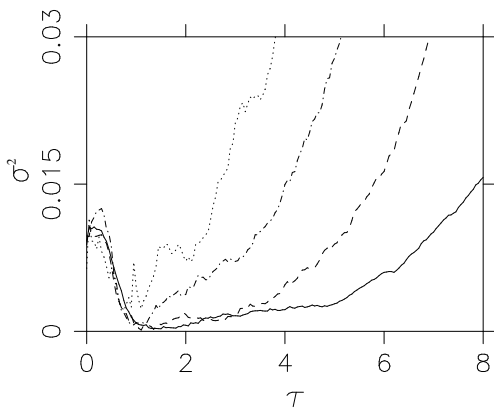$$x_n = N|a_n|^2/\tilde{I}_\tau(E_n), \quad (9)$$

FIG. 2: Variance from the Porter–Thomas results of the wave function intensity distribution for the scar spectrum of Fig.1, calculated using the first 1000 (dotted), 2000 (dotted–dashed), 4000 (dashed), and 8000 (full line) states of the scar spectrum of Fig. 1.

where, coherently with eq. (8), the number of states in the spectrum, N, has been included, in order to obtain a mean value of unity. In Ref. 14 it was shown that this task can be performed systematically by monitoring the corresponding variance from the PT distribution, σ^2, as a function of the smoothing time.

In Fig. 2 we show the results of this calculation when using the first 1000, 2000, 4000, and 8000 states of the scar spectrum of Fig. 1. In order to eliminate the contribution from the tail of the distribution [15] and the divergence at the origin of the PT expression, only values in the range $1 < x_n < 5$ have been included in our statistical treatment. As can be seen, all curves fall off initially quite rapidly as τ increases, and then start to stabilize at $\tau \simeq 1$, indicating that, at least, an optimal fitting to the PT surmise can be obtained when substracting from the intensity distribution the low resolution envelope corresponding to the dynamics of the horizontal PO. This result is in agreement with the conclusions of [15]. It is worth to emphasize that the value of τ for which the PT statistics starts to work is not directly related to the period of the orbit. For instance, for an orbit with a very small Lyapunov exponent, the value of τ would be much greater than 1. More interesting is that, after this point, more optimal values of σ^2 are obtained for a range of values of τ, which extend in some sort of plateau or broad minimum. Finally, the variance grows (approximately) parabolically after a point $\tau_{\max}$, indicating when we are trying to describe the spectrum with too much "dynamical" resolution (for the number of states that have been included in the statistics). The relevance of this figure is that it shows the existence of plateaus, whose extension grow with N. Actually, $\tau_{\max}$ is found to scale, similarly to the Heisenberg time, with $\sqrt{N}$, although it differs from this expression by a factor of $\simeq 10$, indicating that our statistical treatment should allow at least 10 states per

band in order to capture the fluctuations implied by the PT distribution.

This result is further illustrated in Fig. 3, where, in addition to that, the relation between $L_{\max}$, the corresponding orbit length, and invariant classical structures is also revealed. To interpret this figure one must take into account that in the stadium, as in any other chaotic system, Gutzwiller's trace formulae, $\rho(k) = \sum_n \delta(k - k_n)$, gives the quantal density of states in terms of information on all POs of the system. This process can be inverted, by Fourier transform, to obtain the classical spectra of orbits, $f(L) = \sum_n \exp(ik_nL)$. Figure 3 shows the square of this magnitude computed for N=1000, 4000 and 8000. The results in the first panel indicate that 1000 states are barely enough to distinguish between the two PO of length $L \simeq 6.5$ plotted in the insets, which on the other hand are fully resolved when N=4000. The central panel shows how 4000 states are able to discern dynamical features up to $L \simeq 9$. And finally, the results of panel three imply that the quantum mechanics of the system up to $L \simeq 16$ can be described with 8000 states.

In order to elucidate which POs, other than the original horizontal one, are responsible for the plateaus observed in Fig. 2, a similar analysis can be performed with the scar spectrum of Fig. 1, by using the following strategy. Instead of the global density of states, $\rho(k)$, we employ now the local (around the horizontal PO in phase space) version of it,

$$\tilde{f}(L) = \sum_n |a_n|^2 \, e^{ik_nL}. \qquad (10)$$

The inclusion of the weights $|a_n|^2$ it is not an irrelevant point, since it implies that, contrary to what happens in Gutzwiller's original trace formula, only POs dynamically linked to the initial one are allowed to enter in our calculations [18]. The corresponding result is presented in Fig. 4, where it is seen that $|\tilde{f}(L)|^2$ presents a series of prominent peaks at multiples of a fundamental length of 4, the length of the horizontal PO along which the packet was initially launched. Moreover, the contribution of other, longer POs is also clearly observed. By considering the lengths of the different POs of the stadium, we have been able to assign each of the (non–trivial) contributing peaks, up to the fourth recurrence of the horizontal orbit; the corresponding POs are presented in the left inset of the figure. Notice that all these POs present some good portion ot their paths overlapping significantly with the initial horizontal PO. Again the degree of resolution of our calculation is related to the maximum value of k included in the spectrum. This is illustrated in the upper right inset to Fig. 4, where a blown up of the fourth recurrence in $|\tilde{f}(L)|^2$, calculated using 1000 and 8000 states of the scar spectrum of Fig. 1, is presented.

One final point, worth mentioning, is the heights of the peaks in Fig. 4. Since they contain information on the
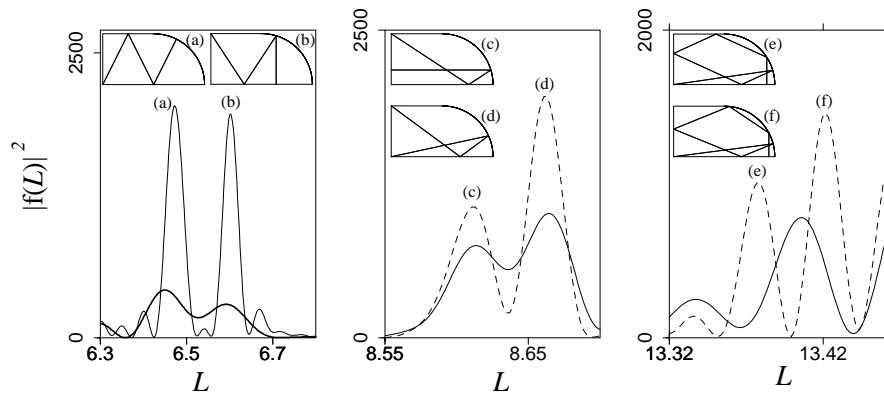
FIG. 3: $|f(L)|^2$ computed from the eigenvalues density of the desymmetrized stadium with Newman boundary conditions for $N=1000$ (thick solid line), 2000 (thin solid line), and 8000 (dashed line), and the corresponding periodic orbits.
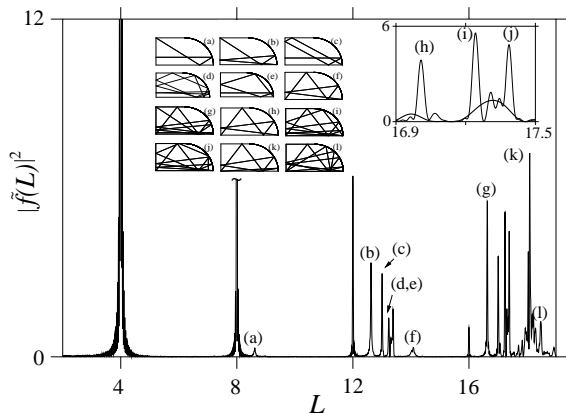

FIG. 4: $|\tilde{f}(L)|^2$ computed from the stick scar spectrum of Fig. 1. The different peaks has been assigned to the periodic orbits plotted in the left inset. The right inset shows how 1000 states (thick solid line) is not enough to reproduce the three central peaks of the fourth recurrence in $|\tilde{f}(L)|^2$.

scales of the corresponding periods.

degree and phase of the interaction between the different POs contributing to $|\tilde{f}(L)|^2$, it must be possible to obtain from them some clue of the scarring process beyond the short time limit corresponding to the linearized dynamics around the initial unstable fixed point. This interaction can be evaluated, for example, as the Hamiltonian matrix elements of the scar wave functions obtained with the methods of Refs. 5, 6, 7, and this will be the subject of a future publication.

In summary, we have shown how scar spectra, containing information about POs dynamically related, can be constructed for highly chaotic systems. This information is revealed by analyzing the associated intensity distributions, which show, superimposed to the universal PT behavior, low resolution structures in the range of time

* Corresponding author: f.borondo@uam.es
[1] F. Haake, *Quantum Signatures of Chaos* (Springer–Verlag, Berlin, 2001).
[2] M. C. Gutzwiller, *Chaos in Classical and Quantum Mechanics* (Springer–Verlag, New York, 1990).
[3] E. J. Heller, Phys. Rev. Lett. **53**, 1515 (1984).
[4] E. J. Heller, in *Chaos and Quantum Physics*, edited by M. J. Giannoni, A. Voros, and J. Zinn–Justin (Elsevier, Amsterdam, 1991).
[5] G. G. de Polavieja, F. Borondo and R. M. Benito, Phys. Rev. Lett. **73**, 1613 (1994).
[6] E. G. Vergini and G. G. Carlo, J. Phys. A. **34**, 4525 (2001); G. G. Carlo, E. G. Vergini and P. Lustemberg, nlin. CD/0204055.
[7] E. G. Vergini, nlin. CD/0205001.
[8] S. Tomsovic and E. J. Heller, Phys. Rev. Lett. **67**, 664 (1991).
[9] S. Tomsovic and J. H. Lefebvre, Phys. Rev. Lett. **79**, 3629 (1997).
[10] T. A. Brody *et al.*, Rev. Mod. Phys. **53**, 385 (1981).
[11] O. Bohigas *et al.*, Phys. Rev. Lett. **52**, 1 (1984).
[12] C. E. Porter and R. G. Thomas, Phys. Rev. **104**, 483 (1956).
[13] Y. Alhassid and R. D. Levine, Phys. Rev. Lett. **57**, 2879 (1986).
[14] E. L. Sibert and F. Borondo, ACH–Models in Chemistry **134**, 595 (1997).
[15] L. Kaplan, Phys. Rev. Lett. **80**, 2582 (1998).
[16] E. Vergini and M. Saraceno, Phys. Rev. E **52**, 2204 (1995).
[17] D. A. Wisniacki, F. Borondo, E. Vergini, and R. M. Benito, Phys. Rev. E **62**, R7583 (2000).
[18] D. A. Wisniacki, F. Borondo, E. Vergini, and R. M. Benito, Phys. Rev. E **63**, 66220 (2001).
[19] D. A. Wisniacki and E. Vergini, Phys. Rev. E **62**, R4513

(2000).